Changes in tumor oxygen state after sorafenib therapy evaluated by ^{18}F-fluoromisonidazole hypoxia imaging of renal cell carcinoma xenografts

WENWEN YU[1,2], SONGJI ZHAO[2-4], YAN ZHAO[5], CHOWDHURY NUSRAT FATEMA[2], MASAHIRO MURAKAMI[2], KEN-ICHI NISHIJIMA[6,7], YOSHIMASA KITAGAWA[1], NAGARA TAMAKI[3,5] and YUJI KUGE[6,7]

[1]Department of Oral Diagnosis and Medicine, Graduate School of Dental Medicine, Hokkaido University, Sapporo, Hokkaido 060-8586; Departments of [2]Tracer Kinetics and Bioanalysis, and [3]Molecular Imaging, Graduate School of Medicine, Hokkaido University, Sapporo, Hokkaido 060-8638; [4]Advanced Clinical Research Center, Fukushima Global Medical Science Center, Fukushima Medical University, Fukushima, Fukushima 960-1295; Departments of [5]Nuclear Medicine and [6]Integrated Molecular Imaging, Graduate School of Medicine, Hokkaido University, Sapporo, Hokkaido 060-8638; [7]Central Institute of Isotope Science, Hokkaido University, Sapporo, Hokkaido 060-0815, Japan

Abstract. A mechanistic dissociation exists between tumor starvation and vascular normalization after antiangiogenic therapy. Thus, improved understanding of tumor responses (tumor starvation or vascular normalization) is important for optimizing treatment strategies. ^{18}F-fluoromisonidazole (^{18}F-FMISO) is widely used for imaging tumor hypoxia. To clarify the tumor response to the antiangiogenic drug sorafenib, the present study evaluated the changes in the tumor oxygen state using ^{18}F-FMISO in mice bearing a renal cell carcinoma xenograft (A498). Mice bearing A498 xenografts were assigned to the control and three sorafenib-treatment groups and administered sorafenib (0, 10, 20 or 40 mg/kg/day, *per os*) once daily for 3 days. Following one day after the final administration, the mice were injected with ^{18}F-FMISO and pimonidazole (a hypoxia marker). ^{18}F-FMISO accumulation in the tumor was determined by autoradiography. Immunohistochemistry of pimonidazole and cluster of differentiation (CD)31 (a vascular marker) was also performed. ^{18}F-FMISO accumulation levels in the tumor significantly increased by 4.3-, 8.4- and 8.6-fold compared with in the control group following 10, 20 and 40 mg/kg sorafenib treatments, respectively [0.07 ± 0.04, 0.32 ± 0.11, 0.62 ± 0.15 and 0.63 ± 0.23 (%ID/m^2) x kg for the control, and 10, 20 and 40 mg treatments, respectively; all $P<0.0083$ vs. the control]. The number of pimonidazole-positive cells also significantly increased by 6.8-, 12.3- and 20.2-fold compared with in the control group following 10, 20 and 40 mg/kg sorafenib treatments, respectively (0.78 ± 0.79, 5.36 ± 2.29, 9.66 ± 1.58 and $15.85\pm4.59\%$ pimonidazole-positive cells; all $P<0.0083$ vs. the control). The number of microvessels in tumors markedly decreased to 33.5, 17.6, and 14.0% of the control following 10, 20 and 40 mg/kg sorafenib treatments, respectively (17.1 ± 2.5, 5.7 ± 1.0, 3.0 ± 1.0 and 2.4 ± 0.3 vessels/mm^2; $P<0.0083$ vs. the control). The ^{18}F-FMISO expression level in the tumor increased sorafenib-dose-dependently, which is consistent with the increase in the number of pimonidazole-positive cells and decrease in the number of microvessels. These findings indicated that the present sorafenib treatment protocol induces 'tumor hypoxia/starvation' in the renal cell carcinoma xenograft (A498) due to its antiangiogenic properties.

Introduction

Angiogenesis is an important hallmark of tumor development and metastasis and is a validated target for cancer treatment (1-3). Sorafenib (BAY 43-9006) is an oral multikinase inhibitor with antiangiogenic properties. Currently, sorafenib has been approved for the treatment of metastatic renal cell carcinoma (RCC) and advanced hepatocellular carcinoma, and is under investigation for use in other malignancies in combination with additional chemotherapies (4).

Conventionally, antiangiogenic drugs inhibit new vessel formation or destroy the tumor vasculature to reduce blood flow and starve the tumor of nutrients (5). However, numerous preclinical studies demonstrated that anti-vascular endothelial growth factor (VEGF) treatment alters the tumor vasculature towards a more 'mature' or 'normal' phenotype ('vascular normalization'), by attenuation of hyperpermeability, improvement of tumor oxygenation and blood flow and the resultant reduction in tumor hypoxia and interstitial

Correspondence to: Professor Songji Zhao, Department of Tracer Kinetics and Bioanalysis, Graduate School of Medicine, Hokkaido University, Kita 15 Nishi 7, Kita-ku, Sapporo, Hokkaido 060-8638, Japan
E-mail: zsi@med.hokudai.ac.jp

fluid pressure (6). These changes can induce an improvement in the metabolic profile of the tumor microenvironment and the efficacy of exogenously administered therapeutics (6). Thus, the mechanistic dissociation between tumor starvation and vascular normalization after antiangiogenic therapy is an important subject in the field of cancer therapy (7). The accurate evaluation of tumor responses after antiangiogenic therapy is of increasing clinical interest and is important for the optimization of treatment protocols (8). With the aforementioned background, improved understanding of tumor responses, such as tumor starvation or tumor vascular normalization, after antiangiogenic therapy is important for optimizing the treatment strategy. ^{18}F-fluoromisonidazole (^{18}F-FMISO) is widely used for imaging tumor hypoxia (9,10). A previous study evaluated the changes in tumor oxygen state following a high-dose (80 mg/kg/day) sorafenib treatment in a RCC xenograft (A498) by ^{18}F-FMISO hypoxia imaging, and the results suggested that the tumor starvation occurs after the sorafenib treatment (11); however, the enhanced intratumoral hypoxia, namely tumor starvation, may be ascribed to the relatively high dose of sorafenib used, as it also decreased the number of tumor microvessels. Thus, the tumor response, such as starvation or vascular normalization, to lower doses of sorafenib treatment is a of great concern and remains to be elucidated.

A previous study revealed that sorafenib decreased the density of intratumoral microvessels and induced a hypoxic state at a high dose (80 mg/kg) in a RCC xenograft (A498) (11). This dose is higher compared with the human clinical dose of 13.3 mg/kg (400 mg/patient twice daily; for example, 13.3 mg/kg for a 60 kg patient) (12). From the findings of this previous study, it is not possible to determine whether this decrease in microvessel density and hypoxic state induction also occur in humans treated with sorafenib, as specific antiangiogenic agents may improve tumor perfusion following their administration at a certain low dose. Thus, the intratumoral responses, such as starvation or vascular normalization, to sorafenib treatment at a clinical dose remain unclear. In the present study, to further clarify the tumor response to the antiangiogenic treatment with sorafenib, the changes in the tumor microenvironment (oxygen/hypoxia states) were evaluated using ^{18}F-FMISO hypoxia imaging following sorafenib treatment at low doses (10, 20 and 40 mg/kg) in the A498 renal cell carcinoma xenograft. The present study aimed to provide information that may lead to an improved understanding of the mechanisms underlying the antiangiogenic effect of sorafenib on renal cell carcinoma and may contribute to the determination of optimum treatment protocols for cancer patients receiving antiangiogenic therapy.

Materials and methods

Radiopharmaceutical and reagents. ^{18}F-FMISO was obtained from the Hokkaido University Hospital Cyclotron Facility (Sapporo, Japan), which was synthesized as previously described (11,13,14). Sorafenib (Nexavar) was purchased from Bayer (Newbury, UK).

Animal studies. The experimental protocol was approved by the Laboratory Animal Care and Use Committee of Hokkaido

University (approval number 13-0057) and performed in accordance with the Guidelines for Animal Experiments at the Graduate School of Medicine, Hokkaido University. Male BALB/c athymic nude mice (n=25, 9-weeks-old; mean body weight, 23.8±1.4 g; Japan SLC, Inc., Hamamatsu, Japan) were used. The room temperature was maintained between 23 and 25˚C and the relative humidity was maintained between 45 and 60%. The institutional laboratory housing provided a 12-h light/dark cycle. Food and water were provided *ad libitum* and met all the criteria of the Association for Assessment and Accreditation of Laboratory Animal Care (AAALAC) International. Fig. 1 presents the experiment protocol of the present study. A human RCC xenograft model was established with the A498 human clear cell RCC (CCRCC) cell line (European Collection of Cell Cultures, Salisbury, UK). A498 cells ($1x10^7$ cells/0.1 ml) were subcutaneously inoculated into the right flank of each mouse. When the tumors grew to 12-13 mm in diameter, the mice were randomly assigned to the control group (n=10) and sorafenib-treated groups (n=15, n=5 for each group; Fig. 1). Mice in the sorafenib-treated groups were further assigned to three groups and treated with 10, 20 or 40 mg/kg sorafenib (n=5 for each group). Sorafenib (10, 20 and 40 mg/kg) in a cremophor EL (Sigma-Aldrich; Merck KGaA, Darmstadt, Germany)/ethanol (Pharmaco Products, Brookfield, CT, USA)/water (12.5:12.5:75) solution was administered daily for 3 days by oral gavage. The cremophor EL/ethanol/water (12.5:12.5:75) solution was administered as the vehicle in the control group. Tumor size was evaluated using a caliper every day from the start of the sorafenib treatment. Tumor volume was calculated using the following formula: π/6 x (largest diameter) x (smallest diameter)^2.

Autoradiography (ARG) with ^{18}F-FMISO. One day after the final sorafenib/vehicle treatment, mice were injected with 18.5 MBq ^{18}F-FMISO followed by pimonidazole (60 mg/kg) after 2 h. Subsequently, 2 h after pimonidazole injection, the mice were sacrificed and the tumors were excised. Each excised tumor tissue was then sectioned at 2-3 mm thickness to maximize the division surface, embedded in Tissue-Tek medium (Sakura Finetek Europe B.V., Flemingweg, Netherlands) with the calf muscle and then frozen in isopentane/dry ice. The frozen specimens were cut into 10-μm-thick cryosections for ARG; four adjacent 5-μm-thick cryosections were used for histological studies.

The distribution of the tracer in the tumor tissue was determined by ARG. Briefly, the cryosections were exposed to a phosphor imaging plate (Fuji Imaging Plate BAS-SR 2025 for ^{18}F; Fuji Photo Film Co., Ltd., Tokyo, Japan) with a set of calibrated standards (15). This autoradiographic exposure was performed overnight to detect the distribution of ^{18}F-FMISO. ARG images were analyzed using a computerized imaging analysis system (FLA-7000 Bio-Imaging Analyzer; Fuji Photo Film Co., Ltd.) with the image analysis software Multi Gauge (Version 3.0; Fuji Photo Film Co., Ltd.).

In order to quantitatively evaluate ^{18}F-radioactivity, regions of interest (ROIs) were selected to cover the entire tumor tissue, excluding the necrotic areas on each ARG image, with reference to the corresponding hematoxylin and eosin (H&E) stained tissue section. The radioactivity in each ROI

was determined by photostimulated luminescence per unit area, PSL/mm^2 (PSL=a x D x t: a=constant; D=radioactivity exposed on the imaging plate; t=exposure time), the percent injected dose per square meter of tissue (%ID/m^2) and normalized with body weight [(%ID/m^2)x kg] were calculated (16,17).

Immunohistochemistry (IHC). The 5-μm-thick cryosections were immunohistochemically stained for pimonidazole and CD31 to assess hypoxia and microvessel density, respectively. Following rehydration and antigen retrieval, endogenous peroxidase activity was blocked for 10 min in 0.1% methanol supplemented with 0.3% hydrogen peroxide. To assess hypoxia, tissue sections were incubated for 60 min with a rabbit polyclonal anti-pimonidazole antibody (cat no. PAb2627AP, Hypoxyprobe; NPI Inc., Burlington, MA, USA) diluted at 1:200 using a Hypoxyprobe-1 Omni kit (Hypoxyprobe, Inc., Burlington, MA, USA). In order to evaluate microvessels, tissue sections were incubated for 30 min with a rabbit polyclonal antibody against CD31 (cat no. ab28364; Abcam, Cambridge, UK) diluted at 1:50. H&E staining at room temperature for 50 min was also performed to assess necrosis.

For the quantitative analysis of hypoxia, the hypoxic fraction, which is the percentage of the cells positive for pimonidazole, as determined by IHC, in the entire cross section (% pimonidazole-positive cells), was determined using ImageJ (Java version 1.6.0; National Institutes of Health, Bethesda, MD, USA). For the quantitative analysis of microvessel density, intratumoral CD31-positive microvessels were counted under an optical microscope (objective magnification, x400; 0.644 mm^2 per field), excluding the peripheral connective tissue and central necrotic tissue, with the analyst blind to the purpose of the present study. Single CD31-positive endothelial cells without any visible lumen were not included in the evaluation. A total of >10 fields per section were randomly analyzed and mean vessel density (MVD, vessels/mm^2) was determined. Necrotic area was evaluated from H&E-stained consecutive sections using ImageJ software.

Statistical analyses. All data are expressed as the mean ± standard deviation. One-factor repeated measures analysis of variance (ANOVA) was performed to compare the tumor volumes of the control group and sorafenib-treated groups. In the evaluation of ^{18}F-FMISO accumulation level, hypoxic fraction, MVD and necrotic area, one-way ANOVA followed by a Bonferroni post hoc test were performed to assess the significance of differences between the control group and sorafenib-treated groups (10, 20 and 40 mg/kg sorafenib treatments). A two-tailed P-value of <0.0083 was considered to indicate a statistically significant difference.

Results

Tumor volume alterations. There was no significant difference in tumor volume between the control group and sorafenib-treated groups during the study period until day 3 (data not shown).

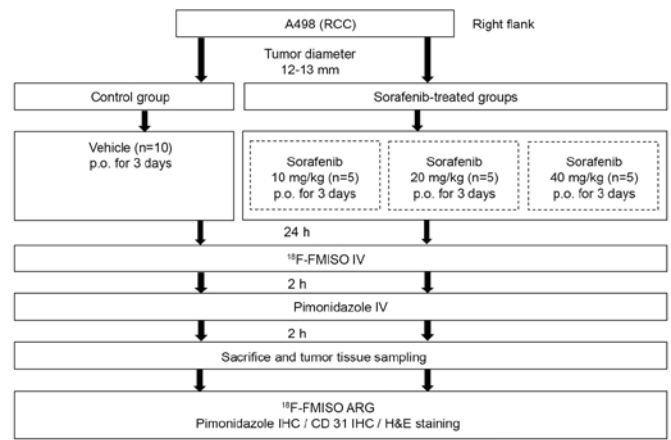*Visual analysis of ^{18}F-FMISO ARG images and histological staining.* The representative images of ^{18}F-FMISO ARG,

Figure 1. Experimental protocol. RCC, renal cell carcinoma; n, number; ^{18}F-FMISO, ^{18}F-fluoromisonidazole; ARG, autoradiography; IHC, immunohistochemistry; H&E, hematoxylin and eosin; CD, cluster of differentiation.

pimonidazole IHC, H&E staining and CD31 IHC are presented in Fig. 2. In the control group, the intratumoral ^{18}F-FMISO distribution was relatively low and the ^{18}F-FMISO expression level was similar compared with that in the muscle tissue, although numerous low ^{18}F-FMISO expression level areas were observed (Fig. 2). In the 10 mg/kg sorafenib-treated group, a number of local spots of high ^{18}F-FMISO expression level were observed in the tumor. The areas with high ^{18}F-FMISO expression level increased with sorafenib dose.

IHC revealed fewer intratumoral pimonidazole-positive areas in the control group (Fig. 2). In the 10 mg/kg sorafenib-treated group, numerous localized pimonidazole-positive areas were observed, which were similar to high-^{18}F-FMISO-expression-level areas (Fig. 2). The pimonidazole-positive areas increased with sorafenib dose, which were similar to the ^{18}F-FMISO ARG results.

H&E staining demonstrated an increase in intratumoral necrotic areas with sorafenib dose (Fig. 2, third panel). Hypoxic areas (high-^{18}F-FMISO-accumulation-level and pimonidazole-positive areas) were observed adjacent to the necrotic areas (Fig. 2, first-third panels).

CD31 IHC revealed a high expression level of CD31 and the abundance of microvessels in the tumor in the control group. The number and density of the microvessels decreased with increasing sorafenib treatment dose (Fig. 2, lower panel).

Quantitative analysis of ^{18}F-FMISO ARG and histological staining. The quantitative evaluation of intratumoral ^{18}F-FMISO accumulation level, hypoxia, necrotic areas and microvessel density are presented in Fig. 3. The intratumoral ^{18}F-FMISO expression levels dose-dependently increased by 4.3-, 8.4- and 8.6-fold compared with that of the control group for the 10, 20 and 40 mg/kg sorafenib treatment groups, respectively (Fig. 3A). The levels of ^{18}F-FMISO expression in tumors were 0.07±0.04 [(%ID/m^2) x kg] in the control group and 0.32±0.11, 0.62±0.15 and 0.63±0.23 [(%ID/m^2) x kg] in the 10, 20 and 40 mg/kg sorafenib-treated groups, respectively (Fig. 3A).

The hypoxia fractions increased by 6.8-, 12.3- and 20.2-fold in the 10, 20 and 40 mg/kg sorafenib-treated groups, respectively, compared with the control group (Fig. 3B). The hypoxia
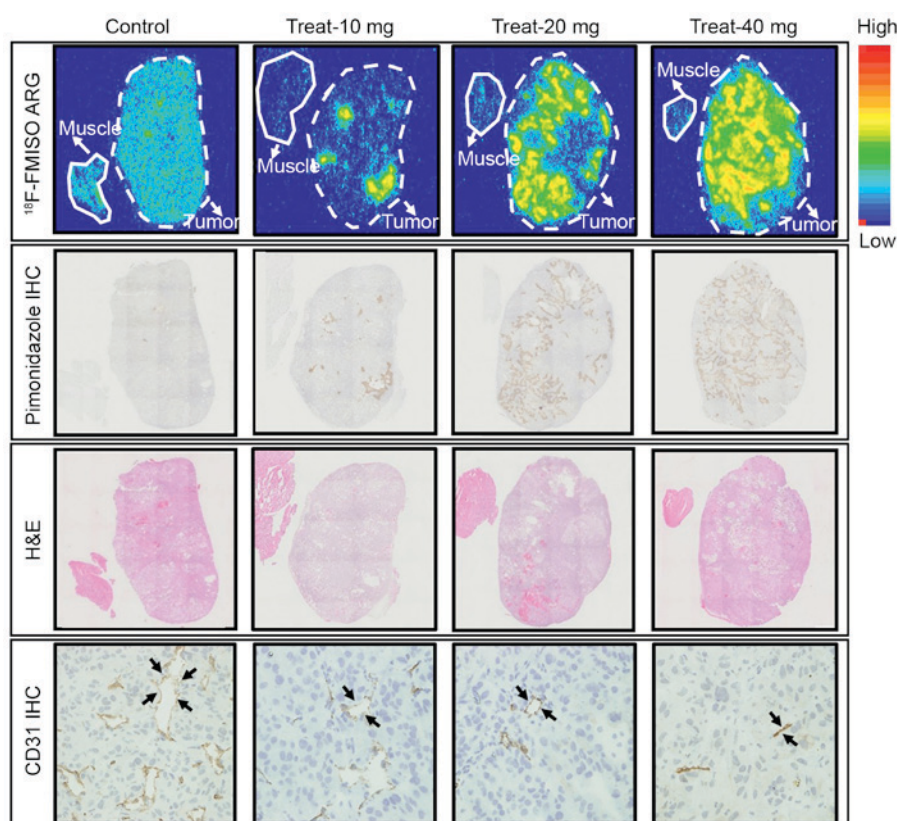
Figure 2. Representative images of ^{18}F-FMISO ARG (upper panel), pimonidazole IHC (second panel), H&E staining (third panel) and CD31 (lower panel). The dotted and solid lines represent the tumor and muscle outlines, respectively. The black arrowheads represent the microvessels. Control, control group; Treat-10 mg, 10 mg/kg sorafenib-treated group; Treat-20 mg, 20 mg/kg sorafenib-treated group; Treat-40 mg, 40 mg/kg sorafenib-treated group. ^{18}F-FMISO, ^{18}F-fluoromisonidazole; H&E, hematoxylin and eosin; ARG, autoradiography; IHC, immunohistochemistry; CD, cluster of differentiation.

fractions in tumors were 0.78±0.79 (% pimonidazole-positive cells) in the control group and 5.36±2.29, 9.66±1.58 and 15.85±4.59 (% pimonidazole-positive cells) in the 10, 20 and 40 mg/kg sorafenib-treated groups, respectively (Fig. 3B).

The necrotic areas in the tumor tissues increased with the dose of sorafenib treatment; however, no significant difference was observed between the control group and sorafenib-treated groups (Fig. 3C). The percentage of necrotic areas in tumor tissues was 3.53±5.13% in the control group and 3.58±2.28, 12.42±8.99 and 10.54±10.29% in the 10, 20 and 40 mg/kg sorafenib-treated groups, respectively (Fig. 3C).

The microvessel densities in the 10, 20 and 40 mg/kg sorafenib-treated groups dose-dependently decreased to 33.5, 17.6 and 14.0% of the control, respectively (Fig. 3D). The microvessel densities in tumors were 17.1±2.5 (vessels/mm^2) in the control group and 5.7±1.0, 3.0±1.0 and 2.4±0.3 (vessels/mm^2) in the 10, 20 and 40 mg/kg sorafenib-treated groups, respectively (Fig. 3D).

Discussion

The major findings of this study were as follows: In the renal cell carcinoma xenograft (A498), the levels of ^{18}F-FMISO expression in the tumor tissues increased sorafenib-dose-dependently, which is consistent with the increase in the number of pimonidazole-positive cells and decrease in the number of microvessels (Figs. 2 and 3). The dose-dependent decrease in the number of microvessels and increase in the tumor hypoxic

fraction in the present study indicated that tumor starvation occurred in the renal cell carcinoma xenograft, as induced by the sorafenib treatment protocol.

According to a previous study and the results of the present study, tumor starvation occurred following sorafenib treatment at a high dose and conventional doses (11). Generally, it is considered that vascular normalization occurs after antiangiogenic therapy at conventional clinical doses or lower doses, although tumor starvation occurs following high-dose or long-term treatment with an antiangiogenic drug. In the present study, sorafenib was administered at doses of 10, 20 and 40 mg/kg. The doses of 10-20 mg/kg are considered to be equivalent to the clinical doses of sorafenib (400 mg/patient twice daily; 13.3 mg/kg for a 60 kg patient) (12). The reasons why tumor starvation occurred in the present study remain unclear; however, this may be ascribed to the characteristics of RCC and the mechanisms underlying sorafenib action. In human CCRCC, A498 is a von Hippel-Lindua (*VHL*) tumor suppressor gene mutant and hypoxia-inducible factor (HIF)-2α is activated, although HIF-1α is absent (18). Mutations or loss of the *VHL* tumor suppressor gene frequently occurs in RCC (19). *VHL*-defective RCC is characterized by high expression levels of HIF-α, which induces overproduction of growth factors, including VEGF and platelet-derived growth factor (PDGF)-β, which activates the membrane-bound receptor tyrosine kinases VEGF receptor (VEGFR) and PDGF receptor (PDGFR) and promotes tumor growth, angiogenesis and metastasis (20). Sorafenib inhibits angiogenesis
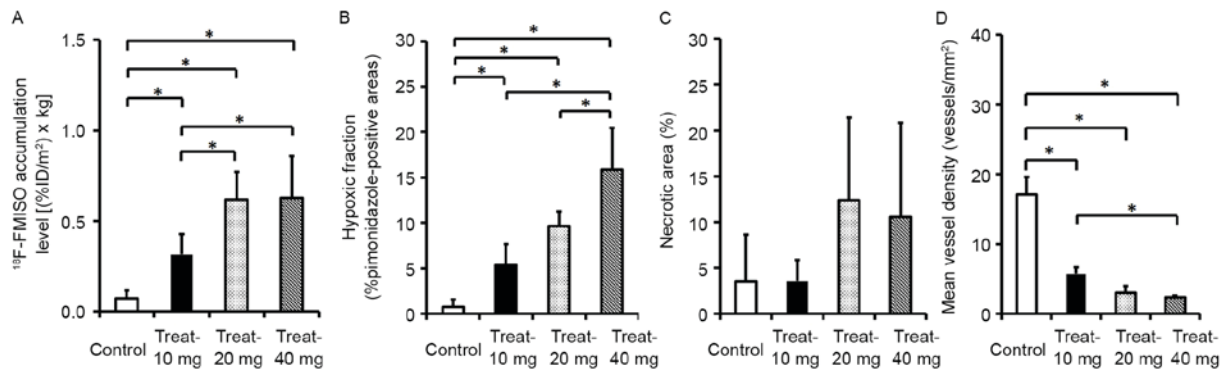
Figure 3. Quantitative analysis of intratumoral (A) ^{18}F-FMISO expression level, (B) percentage of pimonidazole-positive cells, (C) percentage of necrotic area and (D) mean vessel density (vessels/mm^2). Data are expressed as the mean ± standard deviation. One-way factorial analysis of variance revealed significant changes in intratumoral ^{18}F-FMISO expression level (A: F=28.259; P<0.0001), percentage of pimonidazole-positive cells (B: F=47.496; P<0.0001) and vessels/mm^2 (D: F=122.780; P<0.0001) among the four groups. No significant differences were observed in the percentage of necrotic area among the four groups (C: F=2.698; P=0.0718). *P<0.0083, by the Bonferroni post hoc test. ^{18}F-FMISO, ^{18}F-fluoromisonidazole; Control, control group; Treat-10 mg, 10 mg/kg sorafenib-treated group; Treat-20 mg, 20 mg/kg sorafenib-treated group; Treat-40 mg, 40 mg/kg sorafenib-treated group.

by decreasing the activities of VEGFR-2, VEGFR-3 and PDGFR-β (21). Sorafenib has a strong antiangiogenic effect with simultaneous suppression of VEGFR and PDGFR; thus, it is markedly effective for RCC treatment. The histological evaluation (vessel density) of the present study supported this hypothesis (Figs. 2 and 3), although the suppression of VEGFR and PDGFR was not evaluated. Therefore, the strong antiangiogenic effect of sorafenib may induce acute tumor hypoxia (tumor starvation) at clinical doses of sorafenib in highly vascularized RCC.

The accurate evaluation of tumor responses, including tumor starvation or tumor vascular normalization following antiangiogenic therapy, is important for optimizing treatment strategies (8). In the A498 renal cell carcinoma xenograft, the early response (tumor starvation) was observed using ^{18}F-FMISO ARG after three days of sorafenib treatment. When an antiangiogenic drug starves tumor cells, it is considered to be an effective monotherapy. Conversely, when an antiangiogenic drug normalizes intratumoral vasculature and improves blood flow, it is considered to have an enhancive effect in combination therapy. Thus, the results of the present study indicated that monotherapy with sorafenib is effective for the treatment of renal cell carcinoma. Escudier et al (12) reported that sorafenib treatment (400 mg twice daily) prolonged progression-free survival in patients with advanced clear cell renal cell carcinoma in a phase III randomized, double-blind, placebo-controlled TARGET trial with 903 patients whose previous standard therapy had failed. However, it should be noted that sensitivity to sorafenib differs between mice and humans due to species differences and different growth rates of tumors. Thus, the findings of the present study require further evaluation in clinical settings. Furthermore, it is important to evaluate the tumor microenvironment in various tumor xenografts, including actual metastatic RCC models after sorafenib treatment. In the future, the present study would like to evaluate the intratumoral changes in actual metastatic RCC models following antiangiogenic treatment. Conversely, it is important to evaluate tumor perfusion changes after treatment with sorafenib, which would provide further information for understanding the association between the intratumoral

hypoxic state and tumor perfusion alterations. Notably, there was a marked decrease in perfusion in the areas where ^{18}F-FMISO expression was observed in a preliminary study with Hoechst intravenous injection in the same xenograft model after 80 mg/kg sorafenib treatment (data not shown).

^{18}F-FMISO ARG and IHC were performed in the present study 24 h following a once daily sorafenib treatment for 3 days; however our previous study demonstrated that the increase in hypoxic fraction and tumor starvation occurred after once daily 80 mg/kg sorafenib treatment for 7 days in RCC (A498) xenograft (11). Further studies with other treatment protocols, including prolonged treatment periods are required. The subsequent effects of sorafenib on tumor growth following the three-day sorafenib treatment are unclear and require further investigation. Sorafenib is a multikinase inhibitor, which not only has an antiangiogenic property, but also inhibits tumor proliferation.

In conclusion, the present study revealed that the intratumoral ^{18}F-FMISO expression levels and the number of pimonidazole-positive cells significantly increased, whereas the number of microvessels in the tumor significantly decreased following sorafenib treatment of RCC (A498) xenografts. These results indicated that, unlike vascular normalization, tumor hypoxia/tumor starvation occurred following sorafenib treatment at high doses and conventional doses in renal cell carcinoma xenograft (A498), which may be due to the antiangiogenic property of sorafenib. The results of the present study may provide important information that may lead to further understanding of the antiangiogenic mechanisms underlying sorafenib action in renal cell carcinoma.

Acknowledgements

References

1. Carmeliet P and Jain RK: Angiogenesis in cancer and other diseases. Nature 407: 249-257, 2000.
2. Jain RK: Normalization of tumor vasculature: An emerging concept in antiangiogenic therapy. Science 307: 58-62, 2005.
3. Ma J and Waxman DJ: Combination of antiangiogenesis with chemotherapy for more effective cancer treatment. Mol Cancer Ther 7: 3670-3684, 2008.
4. Takimoto CH and Awada A: Safety and anti-tumor activity of sorafenib (Nexavar) in combination with other anti-cancer agents: A review of clinical trials. Cancer Chemother Pharmacol 61: 535-548, 2008.
5. Folkman J: Tumor angiogenesis: Therapeutic implications. N Engl J Med 285: 1182-1186, 1971.
6. Goel S, Duda DG, Xu L, Munn LL, Boucher Y, Fukumura D and Jain RK: Normalization of the vasculature for treatment of cancer and other diseases. Physiol Rev 91: 1071-1121, 2011.
7. Offermanns S and Rosenthal W: Encyclopedia of Molecular Pharmacology. 2nd edition. Berlin, Springer-Verlag, 2008.
8. Oehler C, O'Donoghue JA, Russell J, Zanzonico P, Lorenzen S, Ling CC and Carlin S: 18F-fluomisonidazole PET imaging as a biomarker for the response to 5,6-dimethylx-anthenone-4-acetic acid in colorectal xenograft tumors. J Nucl Med 52: 437-444, 2011.
9. Lawrentschuk N, Poon AM, Foo SS, Putra LG, Murone C, Davis ID, Bolton DM and Scott AM: Assessing regional hypoxia in human renal tumors using 18F-fluoromisonidazole positron emission tomography. BJU Int 96: 540-546, 2005.
10. Eschmann SM, Paulsen F, Reimold M, Dittmann H, Welz S, Reischl G, Machulla HJ and Bares R: Prognostic impact of hypoxia imaging with 18F-misonidazole PET in non-small lung cancer and head and neck cancer before radiotherapy. J Nucl Med 46: 253-260, 2005.
11. Murakami M, Zhao S, Zhao Y, Chowdhury NF, Yu W, Nishijima K, Takiguchi M, Tamaki N and Kuge Y: Evaluation of changes in the tumor microenvironment after sorafenib therapy by sequential histology and 18F-fluoromisonidazole hypoxia imaging in renal cell carcinoma. Int J Oncol 41: 1593-1600, 2012.
12. Escudier B, Eisen T, Stadler WM, Szczylik C, Oudard S, Siebels M, Negrier S, Chevreau C, Solska E, Desai AA, *et al*: Sorafenib in advanced clear-cell renal-cell carcinoma. N Engl J Med 356: 125-134, 2007.
13. Tang G, Wang M, Tang X, Gan M and Luo L: Fully automated one-pot synthesis of [18F] fluoromisonidazole. Nucl Med Biol 32: 553-558, 2005.
14. Oh SJ, Chi DY, Mosdzianowski C, Kim JY, Gil HS, Kang SH, Ryu JS and Moon DH: Fully automated synthesis of [18F] fluoromisonidazole using a conventional [18F] FDG module. Nucl Med Biol 32: 899-905, 2005.
15. Zhao S, Kuge Y, Mochizuki T, Takahashi T, Nakada K, Sato M, Takei T and Tamaki N: Biologic correlates of intratumoral heterogeneity in 18F-FDG distribution with regional expression of glucose transporters and hexokinase-II in experimental tumor. J Nucl Med 46: 675-682, 2005.
16. Brown RS, Leung JY, Fisher SJ, Frey KA, Ethier SP and Wahl RL: Intratumoral distribution of tritiated fluorodeoxyglucose in breast carcinoma. I. Are inflammatory cells important? J Nucl Med 36: 1854-1861, 1995.
17. Toyama H, Ichise M, Liow JS, Modell KJ, Vines DC, Esaki T, Cook M, Seidel J, Sokoloff L, Green MV and Innis RB: Absolute quantification of regional cerebral glucose utilization in mice by 18F-FDG small animal PET scanning and 2-14C-DG autoradiography. J Nucl Med 45: 1398-1405, 2004.
18. Shinojima T, Oya M, Takayanagi A, Mizuno R, Shimizu N and Murai M: Renal cancer cells lacking hypoxia inducible factor (HIF)-1alpha expression maintain vascular endothelial growth factor expression through HIF-2alpha. Carcinogenesis 28: 529-536, 2007.
19. Iliopoulos O, Kibel A, Gray S and Kaelin WG Jr: Tumour suppression by the human von Hippel-Lindau gene product. Nat Med 1: 822-826, 1995.
20. Kaelin WG Jr: Molecular basis of the VHL hereditary cancer syndrome. Nat Rev Cancer 2: 673-682, 2002.
21. Wilhelm SM, Carter C, Tang L, Wilkie D, McNabola A, Rong H, Chen C, Zhang X, Vincent P, McHugh M, *et al*: BAY 43-9006 exhibits broad spectrum oral antitumor activity and targets the RAF/MEK/ERK pathway and receptor tyrosine kinases involved in tumor progression and angiogenesis. Cancer Res 64: 7099-7109, 2004.